LA-5727-PR
Progress Report

Applied Nuclear Data
Research and Development
Quarterly Progress Report

April 1 through June 30, 1974

Edited by

G. M. Hale
D. R. Harris
R. E. MacFarlane

los alamos
scientific laboratory
of the University of California
LOS ALAMOS, NEW MEXICO 87544

This report presents the status of the Applied Nuclear Data Research and Development Program. Other reports in this series, all unclassified, are:

LA-5546-PR   LA-5570-PR   LA-5655-PR

In the interest of prompt distribution, this progress report was not edited by the Technical Information staff.

CONTENTS

Items I, III, IV, VI, VII, VIII, X, and XI include work for
DRRD. Items I, III, IV, VI, VII, VIII include work for DMA.
Items VI and VIII include work for DNA. Items I and V include
work for DCTR. Items I, II, IV, and XI include work for DRSR.
Item IX is work for NASA.

APPLIED NUCLEAR DATA RESEARCH AND DEVELOPMENT

QUARTERLY PROGRESS REPORT

April 1 through June 30, 1974

Edited by

G. M. Hale, D. R. Harris, and R. E. MacFarlane

ABSTRACT

This report presents progress in provision of nuclear data for nuclear
design applications. The work described here is carried out through the LASL
Applied Nuclear Data Group and covers the period April 1 through June 30, 1974.
The topical content of this report is summarized in the Contents.

I. NUCLEAR CROSS-SECTION PROCESSING (R. E. MacFarlane, T. R. England, D. G. Foster, Jr., J. H. Hancock, D. R. Harris, R. J. LaBauve, D. W. Muir, and N. Whittemore)

Group T-2 is supporting and developing a variety of computer codes for processing evaluated nuclear data into forms that can be used for design purposes. The groups' capabilities include multigroup neutron, gamma production, and gamma interaction cross sections; pointwise cross sections for continuous energy Monte Carlo codes; and a variety of data management, plotting, and format conversion functions. The following subsections summarize recent progress.

A. Cross-Section Production

During this quarter, multigroup cross sections for Li-6 (ENDF/B-III MAT 1115) and Li-7 (ENDF/B-III MAT 1116) and pointwise cross sections for ^{235}U (ENDF/B-IV preliminary MAT 25) and ^{238}U (ENDF/B-IV preliminary MAT 238) were generated for the Los Alamos Scientific Laboratory (LASL) theoretical design division using MINX. Multigroup cross sections for iron (DNA MAT 4180 MOD 2) were processed for the radiotherapy shield project described last quarter.[1] Multigroup cross sections in the 239 group structure[2] and Version II CCCC format[3] were produced for ENDF/B-III ^{16}O, Fe, and ^{23}Na (MATS 1134, 1180, and 1156). These results will form part of a preliminary CCCC library which will be used by Westinghouse Advanced Reactor Development (WARD) to test the MINX-SPHINX

interface. Multigroup cross sections for vanadium and niobium (ENDF/B-III MATS 1017 and 1203) were processed for the LASL CTR library, and copper and gold (ENDF/B-III MATS 1087 and 1166) were processed for the Chemistry and Nuclear Chemistry Division.

B. MINX Validation

A revision of the TEDIUM[4] to ENDF/B-IV standards has been completed. The new deck has been sent to Oak Ridge National Laboratory (ORNL) for comparison with SUPERTOG and the ORNL version of MINX. Additional comparisons with the LASL versions of MINX and ETOX are being carried out here.

C. MINX Code Development

A number of code changes were made this quarter to correct errors found while processing new materials or to increase the usefulness of the code. The changes in Doppler broadening and in the treatment of the ENDF/B-IV fission representation are discussed in subsections D and E. New additions to the code include an option to restart from a zero degree pointwise tape without repeating resonance reconstruction, an option to compress any group structure for materials with a maximum energy of 15 MeV, and a GAM-I group structure option. The RESEND section of MINX was modified to include the energies for the unresolved resonance parameters in the energy grid and to set any negative cross sections generated to zero. The subroutine for computing secondary energy distri-

butions by LAW9[5] was modified to improve its precision, and the treatment of multiple secondary energy distributions (as in iron MAT 1180) was modified to reduce storage requirements. To improve the running time for complicated resonance materials such as ^{238}U, the Doppler broadening module was modified. In the current version, thinning is performed in the resolved resonance region only. The thinned broadened tape is then used as the starting point for the next broadening operation. This decreases the time required for broadening significantly.

D. Doppler Broadening of Pointwise Cross Sections

The MINX processor uses the kernel broadening method[6] to compute temperature dependent cross sections. It has been observed that the Doppler broadening is not accurate for low energies and high temperatures. In fact, negative cross sections are sometimes produced. This problem has been traced to a loss of precision in the calculation of the function

$$H_n(a,b) = \int_a^b z^n e^{-z^2} dz$$

$$= \int_a^\infty z^n e^{-z^2} dz - \int_b^\infty z^n e^{-z^2} dz$$

when a is close to b. The Doppler broadening module in MINX has been modified to detect this loss of significance. In such a case, it computes $H_n(a,b)$ by a direct Taylor expansion of the integral which converges rapidly if a is close to b. The new method preserves the $1/v$ cross section down to 10^{-5} eV for temperatures as high as 12,000,000°K.

E. Treatment of ENDF/B-IV Fission Representation

Earlier versions of the ENDF/B evaluated nuclear data files have represented the energies of the secondary neutrons from fission using Maxwellian "evaporation" distributions. The characteristic temperatures for the distributions do not change very much with incident neutron energy. This makes it practical to represent the fission neutrons by a single "fission spectrum." Although this is a good approximation for most reactor problems, at high energies the fission spectrum becomes more strongly dependent on the energy of the incident neutron.

In order to make ENDF/B-IV useful for systems with a thermonuclear neutron spectrum, the partial fission reactions MT 19, 20, 21, and 38 have been activated. The reaction represented by MT 19 is fission of the compound nucleus following neutron absorption and the Maxwellian distribution is used. The other three partial reactions are represented as scattering processes (n-n', n-2n, and n-3n) followed by fission of the residual nucleus. The secondary energy distribution of the "scattered" neutrons are represented by a partial energy distribution in File 5 appropriate to the type of scattering. The neutrons from the fission of the residual nucleus are represented by a second partial energy distribution chosen to be the same Maxwellian used in MT 19.

The problem for the processing code is how to represent this increased complexity. The most general answer is to use the full fission matrix including up-scatter. However, this could be very costly in storage and running time for the discrete ordinates transport codes usually used in this energy range. For this reason, MINX has been modified to divide the fission transfer into two parts. The "evaporation" neutrons are processed into a fission spectrum as in previous versions. The "scattering" neutrons are processed into transfer matrices and added into the total scattering matrix. The function $\overline{\nu\sigma}_f$ used to compute the fission source in the transport code refers to the "evaporation" fraction of the fission neutrons only. The transport code can then be used to compute the correct flux in the usual manner. When the solution has been completed, the user must be careful to use the correct fission cross section in computing the fission reaction rate. This representation of the fission reaction is consistent with most transport codes and doesn't require the storage and use of up-scatter matrices.

F. MINX-II Code Development

A strength of MINX-II is its extremely modular structure. A major module in the treatment of group-to-group transfer matrices is the one which calculates the "feed function," that is, the probability that a neutron at source energy E will cause a neutron or gamma ray to appear in sink group g'. The concept of the feed function allows all neutron and gamma production cross sections and transfer matrices to be computed by the same integration routine. A preliminary module has been written to calculate the feed function for elastic and discrete inelastic scattering when the Legendre expansions are given in the laboratory coordinate system (this

case can be done analytically by the method used in MINX-I). Since the feed function contains structure which does not occur in the cross section, the module generated additional energy points to be included in the subsequent integration over source energy. The points are generated using a minimal grid stack and in such a way as to preserve maximum flexibility in the order of looping on source grid, sink group, and Legendre order.

II. HTGR SAFETY PROGRAM (D. R. Harris, R. J. La Bauve, T. R. England, and P. D. Soran [T-1])

A. Thermal Neutron Cross Sections

Multigroup cross sections for use in HTGR neutronic calculations are being generated from the ENDF/B basic data file. The group structure being used for initial loading calculations is shown in Table I. At present, the MC^2 code[7] is being used to generate all cross sections for all absorber nuclides and for the epithermal cross sections of the graphite moderator. (Future plans[8] call for the use of the MINX-SPHINX[9] codes when the SPHINX code becomes operational at LASL.)

In order to facilitate the operation of the MC^2 code, especially since cross sections are needed for several temperatures, all preprocessing and peripheral codes related to MC^2 have been linked on the CDC-7600. The flow of data through this linked MC^2 system is shown in Fig. 1. The RIGEL[10] code is used

TABLE I

GROUP STRUCTURE USED
FOR INITIAL HTGR SAFETY STUDIES

E_{max} = 10.0 MeV

Group No.	E_{Lower}	Lethargy	Delta U
1	6.065 MeV	0.50	0.50
2	4.724	0.75	0.25
3	2.865	1.25	0.50
4	1.738	1.75	0.50
5	1.054	2.25	0.50
6	0.302	3.50	1.25
7	0.183	4.00	0.50
8	0.111	4.50	0.50
9	0.041	5.50	1.00
10	0.960 keV	9.25	3.75
11	0.017	13.25	4.00
12	3.928 eV	14.75	1.50
13	2.383	15.25	0.50
14	0.414	17.00	1.75
15	0.092	18.50	1.50
16	0.044	19.25	0.75
17	0.008	20.00	1.75

to convert an ENDF/B data tape in standard, BCD format (Mode 3) to alternate, binary format (Mode 2). The ETOE[11] code prepares a library tape for MC^2 which includes "W-tables" supplied by the code WLIB. Note that since the ETOE code provides pointwise elastic scattering cross sections for MC^2, the temperature is an input parameter of ETOE. Consequently, a different MC^2 library tape must be prepared for each temperature. Not shown in the figure but also available in the MC^2 code system is the MERMC2 code. This code can be used for merging MC^2 library tapes.
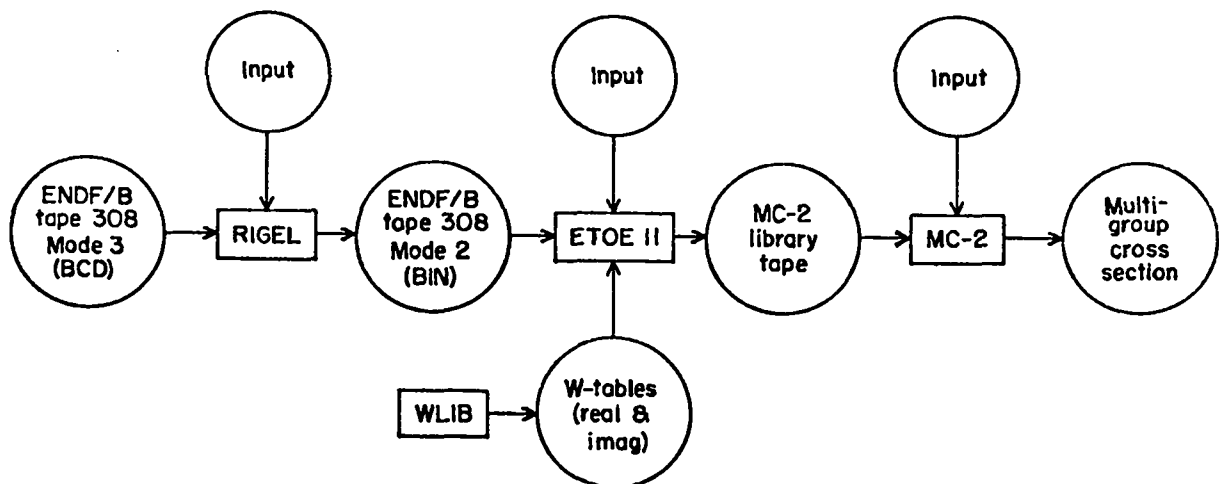

Fig. 1. MC^2 code system (LASL CDC-7600 Version).

The MC^2 code is being used in a rather restricted sense for this initial HTGR work. First, because of storage limitations, cross sections for the entire energy range cannot be generated in one pass, so separate, but overlapping, problems are run for the "high" energy range and "low" energy range. Second, only the "all fine" option is being used in MC^2 with fine group spacings of 0.25 in lethargy. The weighting specified for the derivation of the fine groups from the pointwise ENDF/B data is "1/E." Third, weighting fluxes for collapsing from fine to broad cross sections are input for both the "high" and "low" energy problems. A "1/E" weighting flux is used for the high-energy problem, and a Maxwellian at the proper temperature plus a 1/E weighting function is used for the low-energy problem. Finally, because of the above limitation, only single table, transport corrected cross sections can be obtained. A small code "JMBLFAT" has been written to combine the high and low energy ranges to produce cross sections in the DTF format. Table II gives a list of nuclides for which cross sections have been obtained to date, along with the version of ENDF/B used for each nuclide.

TABLE II

HTGR NUCLIDES FOR WHICH
CROSS SECTIONS WERE GENERATED FROM MC^2

(T = 300°K)

Nuclide	MAT No.	ENDF/B Version
Th-232	1117	3
Pa-233	1119	3
U-235	1157	3
U-238	1158	3
C-12	1165	3
O-16	1134	3
Fe	1020	1
Cr	1018	1
Ni	1021	1
Sm-149	1027	1
Xe-135	1026	1
U-236	1046	1
U-233	1041	1
U-234	1043	1

Two sets of codes are being used to produce thermal cross sections for the graphite moderator. The first of these consists of using the Los Alamos codes TOR[12]-GLEN.[13] The other approach consists of using the FLANGE[14] code to process the thermal data from ENDF/B. The data on ENDF/B was generated by the General Atomic (GA) code GASKET,[15] and this sec-

ond calculational approach will enable us to compare the results of the Los Alamos codes with those from codes developed at GA.

B. ^{135}Xe-Power Stability

The conclusions regarding the asymptotic stability in the Fulton Plant PSAR[16] were examined using an improved analysis[17,18] which results in the following conditional equation:

$$\Delta\lambda > \frac{\eta(\gamma_I - \gamma_{Xe})}{\nu'(1+\eta)(1+c+\eta)+(\eta\gamma_I - \gamma_{Xe})}$$

where

$$\Delta\lambda \equiv \lambda_0 - \lambda_1 \quad ,$$

the difference between the fundamental and first overtone flux eigenvalues,

$$\eta \equiv \frac{\bar{\phi}_{th}\bar{\sigma}_{Xe}}{\lambda_{Xe}}$$

$\bar{\phi}_{th}$ = average thermal flux

$\bar{\sigma}_{Xe}$ = average ^{135}Xe cross section

λ_I, λ_{Xe} = decay constants for ^{135}I and ^{135}Xe

$c \equiv \lambda_I/\lambda_{Xe}$

ν' = ν times a ratio of the adjoint weighted values of a few-group vs one-group fission matrix (ν varies from ~ 1.5 to 2.0 in power reactors; in a one-group treatment, it would be ~ 2.43)

γ_I, γ_{Xe} = ^{135}I cumulative yield and ^{135}Xe independent yield.

The computed $\Delta\lambda$ is a necessary minimum value for asymptotic stability in the absence of temperature feedback. The expression involves several approximations to the fundamental modal equations which are derived from the equations of state coupling the ^{135}I \rightarrow ^{135}Xe chain to the neutron flux groups. However, the above expression for a minimum $\Delta\lambda$ is generally more accurate than the ν' and η parameters.

For the Fulton Plant we used an η equal to 9; this value, derived from the average Fulton Plant flux value, requires additional verification. In

addition, the conclusions from our analysis require a verification of the overtone eigenvalues, particularly over the reactor lifetime. Although GA apparently now has one-dimensional overtone calculations, the $\Delta\lambda$'s we infer from data in the Fulton Plant PSAR are likely not based on such calculations. The $\Delta\lambda$'s are larger than one would expect from a plant having an effective core *size* of ~ 8.5 x 6.4 m. This was discussed at GA with W. Simon and A. Baxter. They indicated a later analysis had been made which could not be released at that time. The difference is crucial to the conclusions and an independent calculation of $\Delta\lambda$ is desirable if the details of the later GA calculations remain unavailable. The analysis results in the values of Table III.

Based on these results we agree with the general conclusion in the PSAR that the Fulton Plant is stable axially and requires a net negative temperature feedback for radial stability; but we emphasize that this agreement, while using an improved stability criterion, is still contingent on the data inferred from the PSAR.

TABLE III

STABILITY PARAMETERS FOR FULTON PLANT[a]

Mode	Inferred from PSAR	Required for Asymptotic Stability
Axial		
No temp feedback	0.03	0.024
With temp feedback	0.048	0.024
Radial		
No temp feedback	0.019	0.024
With temp feedback	0.037	0.024

[a]Where the temperature feedback alters $\Delta\lambda$ by 0.018 based on PSAR Table 4.3.2-13.

C. HTGR Decay Heat Analysis

At GA's request the report on HTGR decay heat[19] was reviewed with particular attention to the analysis of uncertainty. The review was discussed at GA with V. Yoksimovic and R. K. Dermer. In general the GA analysis was reasonably thorough but the small un-

certainty assignments were not justifiable. The GA analysis, like all other existing analyses, will be made obsolete following general use of the new, more extensive ENDF/B-IV data files and inclusion of absorption effects.

III. DELAYED γ-SPECTRA FOR PHOTONEUTRON PRODUCTION (T. R. England)

The delayed γ-spectrum has been computed for ^{235}U and ^{239}Pu thermal fission and for ^{238}U and ^{239}Pu fast fission. Sixty-six groups in 50 keV intervals were used beginning at 1.67 MeV. Results apply following ~ 1/2 h of cooling and cover the photoneutron production energy range for ^{9}Be and deuterium (threshold energies are 1.67 and 2.23 MeV, respectively). The spectrum was calculated at 28 time intervals beginning at 1 h and extending to 1000 h following a constant fission period of one month. The calculation includes all known fission products having a half-life $\gtrsim$ 15 min which emit γ's above 1.67 MeV, and only the γ energies and intensitites above this value were included—approximately 17 lines per nuclide on the average. ENDF/B-IV yields and branching ratios were used. The accuracy of these calculations is determined only by experimental data for nuclide parameters; there is no approximation.

Figures 2-5 show the spectrum for $^{235}U + n_{th}$ at 1, 10, 100, and 1000 h following the one month irradiation period. Each histogram is normalized to the total γ's/fission at the respective times over the interval 1.67 → 5.0 MeV. Normalization values are given on each plot. Interestingly, the four histogram plots indicate that the spectrum hardens with time.

Figures 6-9 show the time dependence over the broad energy ranges of 1.7 → 5.0, 1.7 → 2.23, and 2.23 → 5.0 MeV normalized to the values at 1 h over these energy ranges. The 2.23 → 5.0 MeV range applies to the (γ,n) reaction in deuterium which is the primary, or only significant, source of photoneutrons in light water reactors in the absence of ^{9}Be. The degradation of this spectrum before the (γ,n) reaction occurs has been shown to be insignificant in earlier studies.

The long period of 10 → 200 h during which the 2.23 → 5.0 MeV source is nearly constant is due primarily to the (12.8d)^{140}Ba decay to (40.23h)^{140}La.
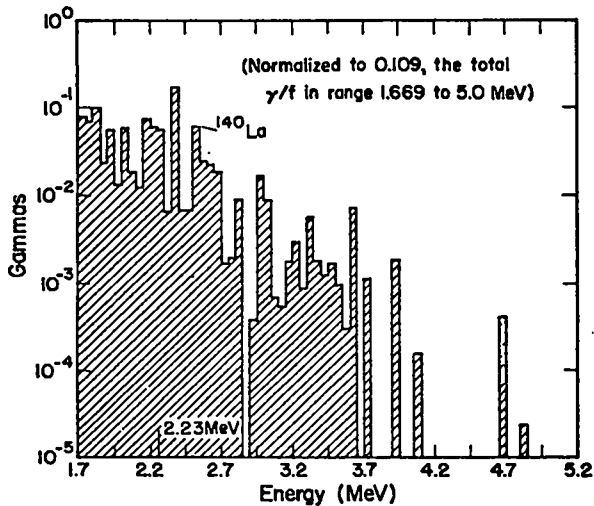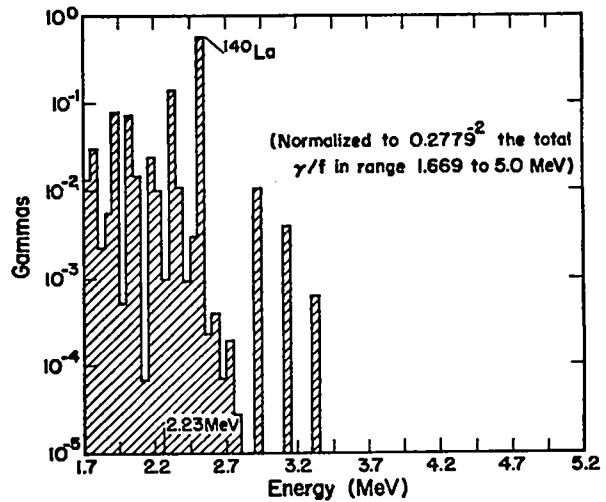
Fig. 2. Gamma spectrum at 1 h for ^{235}U thermal fission.
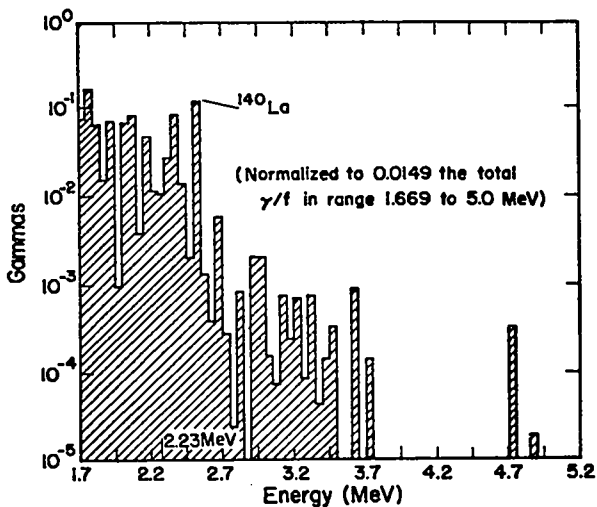

Fig. 4. Gamma spectrum at 100 h for ^{235}U thermal fission.

Fig. 3. Gamma spectrum at 10 h for ^{235}U thermal fission.

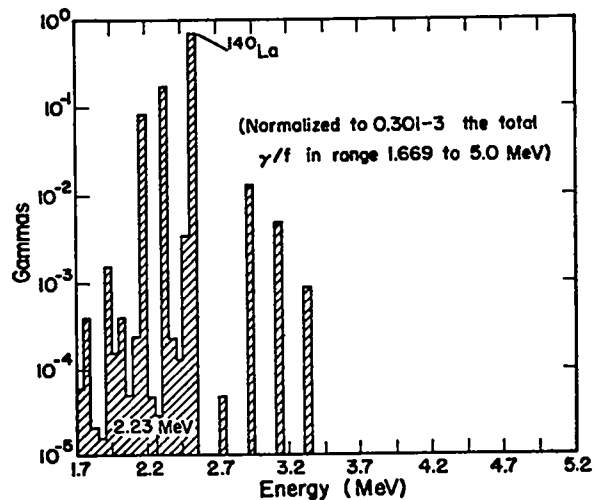Fig. 5. Gamma spectrum at 1000 h for ^{235}U thermal fission.

^{140}Ba does not emit photoneutrons above the (γ,n) threshold of deuterium, but ^{140}La, the emitter, is in transient equilibrium with the relatively long-lived ^{140}Ba precursor. Its most intense γ occurs in the 2.5 → 2.55 MeV bin as noted on the histogram plots. Its contribution to this bin changes only ~ 9% between 10 and 100 h.

One obvious conclusion from these results is of practical interest in sourceless startups of light water reactors: assuming external detectors can accurately determine reactivity following approximate-

ly a 10-h shutdown, then measurements following a week or more should be equally valid.

IV. ENDF/B-IV DECAY DATA (T. R. England)

A. Delayed Neutron Calculations Based on ENDF/B-IV Data

The previous progress report[1] covered delayed neutron yields (d.n.y.) calculations in detail based on nuclide fission yields and neutron emission probabilities. Precursor parameters were included in the previous report. Calculations have been continued. Table IV lists the calculations and ENDF/B-IV
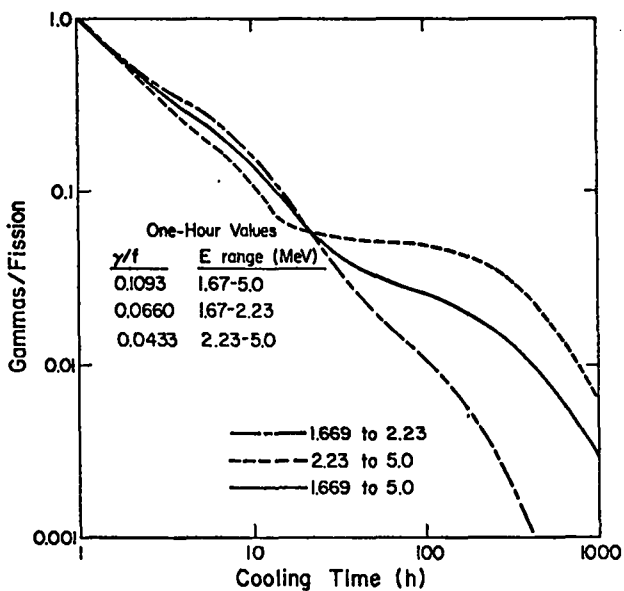
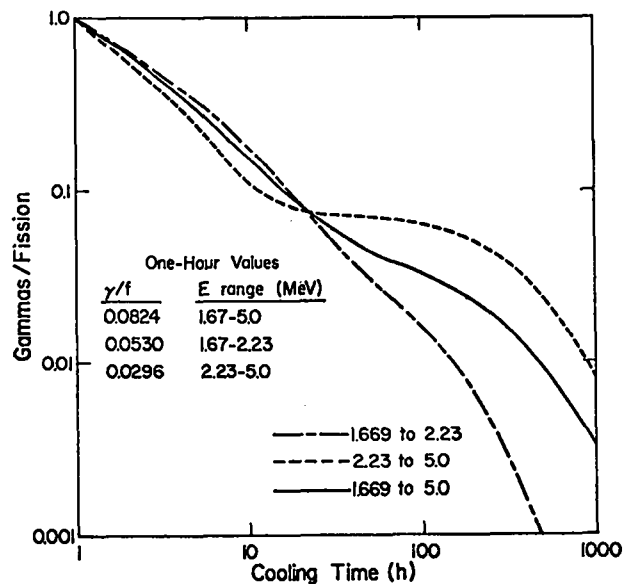Fig. 6. Gammas per fission vs cooling time over 3 energy ranges for [235]U thermal fission.

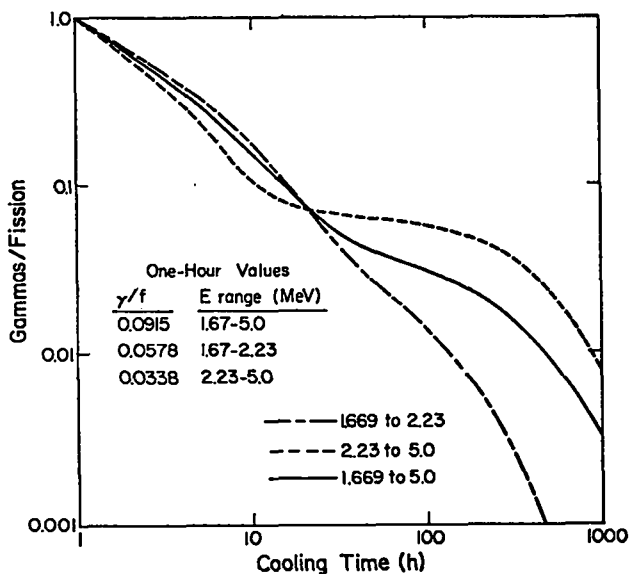Fig. 8. Gammas per fission vs cooling time over 3 energy ranges for [239]Pu thermal fission.

Fig. 7. Gammas per fission vs cooling time over 3 energy ranges for [235]U fast fission.
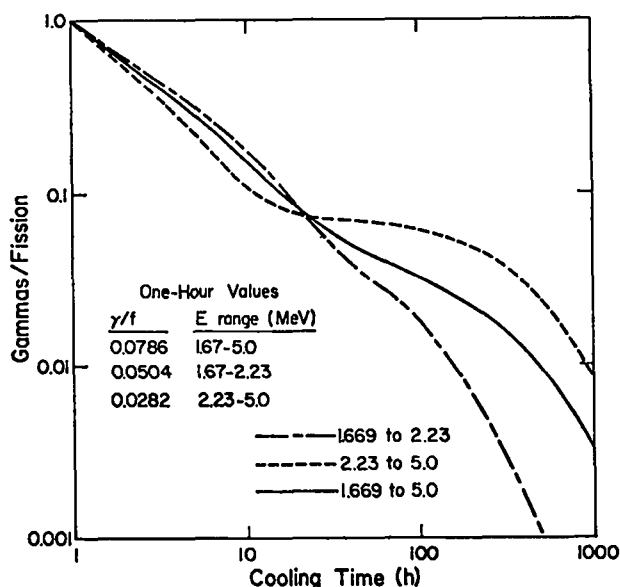

Fig. 9. Gammas per fission vs cooling time over 3 energy ranges for [239]Pu fast fission.

evaluated d.n.y.'s for all fissionable nuclides and neutron fission energies for which precursor yield information in the decay files (10 yield sets). The sensitivity of d.n.y.'s to yield model parameters was noted in the previous progress report. Column B of Table IV used the cumulative chain yields in ENDF/B-IV, but the fractional yields are estimated entirely by the yield distribution model without using an even-odd Z dependence. Column C uses

± 25% even-odd Z dependence. Column C uses a ± 25% even-odd Z dependence and Column A uses the Pn and fractional yields in ENDF/B-IV files. The interesting features of these calculations are:

1. Model estimated fraction of cumulative yields without an even-odd Z dependence provides better agreement with evaluated d.n.y.'s than use of the ENDF/B-IV evaluation of cumulative yields.

TABLE IV

TOTAL DELAYED NEUTRON YIELDS PER 10000 FISSIONS

Nuclide	ENDF/B-IV Evaluation[a]	ν_d Calculated A	B	C
$U^{235}T$	166.8 ± 7.	157	168	133
$U^{235}F$	166.8 ± 7.	110	165	136
$U^{235}HE$	90.0 ± 10.	123	117	–
$U^{238}F$	460.0 ± 25.	309	328	284
$U^{238}HE$	260.0 ± 20.	171	–	–
$Pu^{239}T$	64.5 ± 4.	56	57	49
$Pu^{239}F$	64.5 ± 4.	32	57	–
$Pu^{241}T$	157.0 ± 15.	98	–	–
$U^{233}T$	74.0 ± 4.	80	–	68
$Th^{232}F$	527.0 ± 40.	295	–	–

[a]Recommended in ANL/NDM-5

Column A: ENDF/B-IV P_n and yields
     B: No Even-Odd Z Effect
     C: Even-Odd Z = ± 25%

2. With or without an even-odd Z dependence, the model estimates agree with experiment in that essentially no energy dependence is observed below the 2nd chance fission threshold.

3. D.n.y. values in Column B for ^{235}U, ^{233}U, and ^{239}Pu agree with evaluation within 0.5 to 11%, the best agreement being for ^{235}U and the worst for ^{239}Pu.

4. ^{238}U, ^{232}Th, and ^{241}Pu are markedly low. This is likely due to the relatively poor knowledge of cumulative yields for these nuclides.

In Table V, the $^{235} + n_{th}$ values are given for each of the conventional 6 groups. The grouping is approximate, the group assignment being made on the basis of nearness of each nuclide half-life to the ENDF/B-IV evaluation. The first four groups are improved by use of model estimated fractional yields and no even-odd Z effect.

One can conclude from these results that the existence of the even-odd Z effect for delayed neutron precursors is questionable or, possibly, that model parameters used in estimating the yield vs charge distribution are in error. The fast yields for ^{232}Th and ^{238}U and the thermal ^{241}Pu yields clearly need improvement. Results for ^{233}U, ^{235}U, and ^{239}Pu are considerably better than one might

TABLE V

^{235}U DELAYED NEUTRONS PER 10000 FISSIONS

Group	ENDF/B-IV γ1/2(sec)	ν_d	ν_d Calculated A	B	C
1	54.51	6.34	5.1	5.2	5.0
2	21.84	35.5	30.4	32.4	28.1
3	6.00	31.4	27.0	23.6	18.4
4	2.23	67.9	62.1	66.6	54.3
5	0.496	21.4	25.7	26.4	0.8
6	0.179	4.3	7.2	13.4	6.1
		166.8 ± 7	157.4	67.6	132.6

Column A: ENDF/B-IV P_n and yields
Column B: No even-odd Z effect
Column C: Even-odd Z effect = ± 25%

have expected; we are clearly approaching the time when one can rely on detailed nuclide calculations for properties of the delayed neutrons rather than on the conventional amalgamation into 6 groups.

B. ENDF/B-IV Decay/Absorption Files

Phase I review of yields has continued during this period. Figures 10-12 show comparisons of several sets of cumulative yields. These are of limited interest; there are ~ 8, nonzero independent (direct) yields at each mass number, and only the independent yields are included in ENDF/B-IV. There are 10 yield sets in the files for the 6 fissionable nuclides and energies as noted in the delayed neutron calculations (Table V). The files list yields for 1019 nuclides per set, even if values are zero, which include the 825 fission products having decay and/or cross-section data in ENDF/B-IV.

Cross-section data for ~ 155 nuclides are being assembled in ENDF/B-IV format by R. Schenter. Approximately 181 products will have cross-section data counting the general purpose file. These data must be sufficient for both thermal and fast reactors. In thermal reactors, absorption calculations generally use ~ 200 nuclides but ~ 20 contribute more than 80% of the total absorption. These were identified by calculations at LASL along with a subsequent Phase I review.
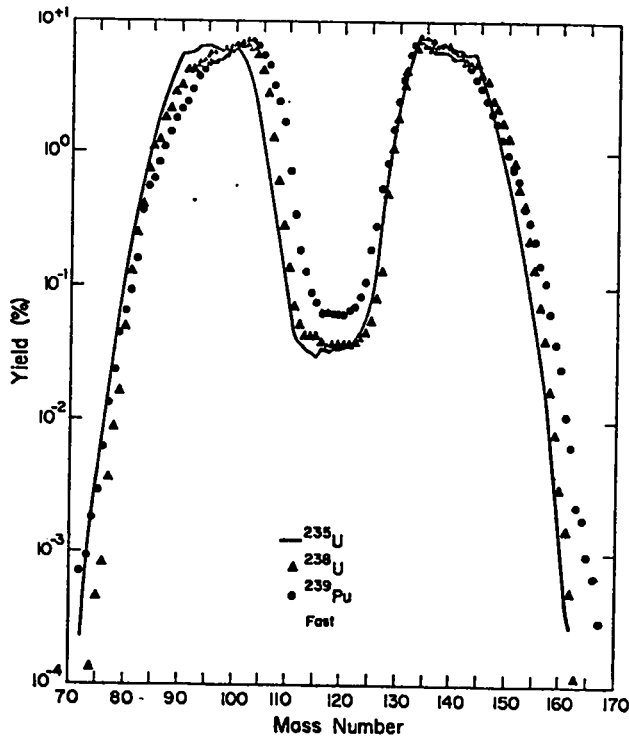
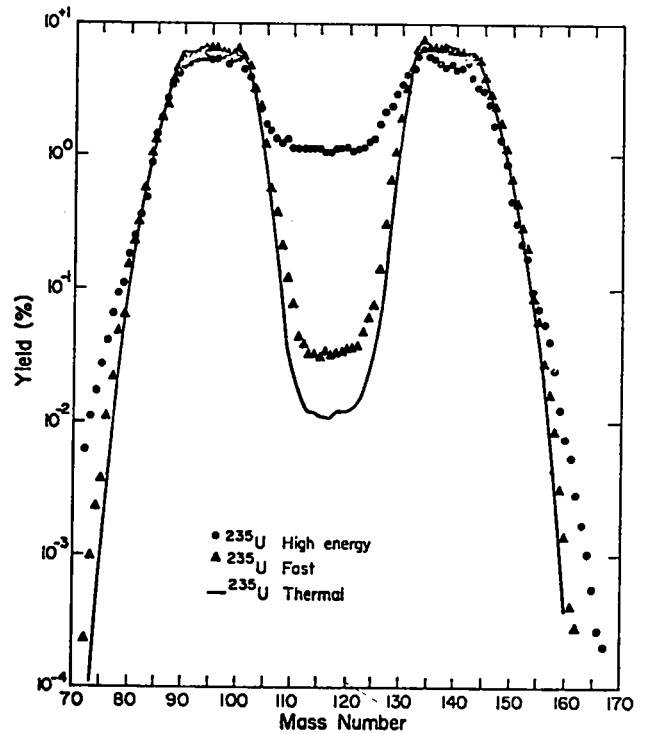Fig. 10. Comparison of mass chain yields, fast fission.

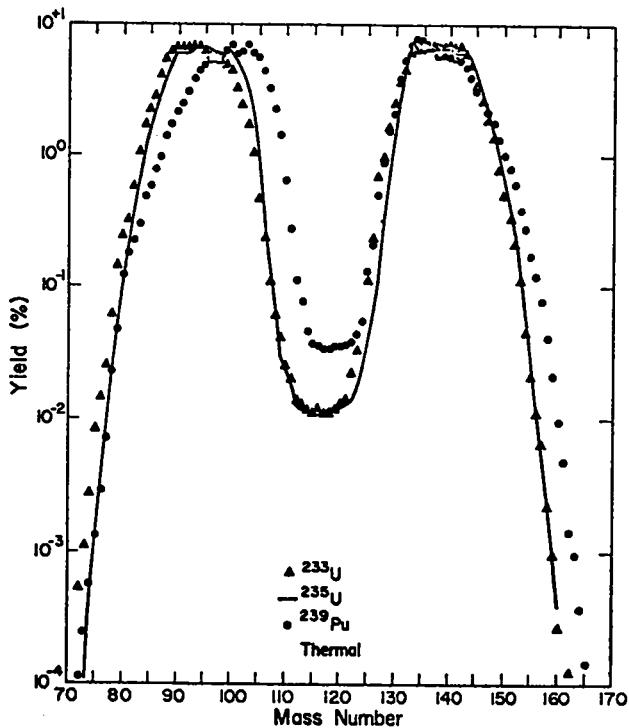Fig. 12. Comparison of mass yields at 3 energies for ^{235}U fission.

Fig. 11. Comparison of mass yield for thermal fission.

V. NUCLEAR DATA FOR THE CONTROLLED FUSION PROGRAM (D. W. Muir, L. Stewart, R. J. LaBauve, D. G. Foster, Jr. and R. E. Seamon [TD-6])

Considerable effort has been devoted in this quarter to the task of preparing multigroup data for the analysis of fusion-fission hybrid reactors. A 25-group structure was formed as a subset of both the LASL/CTR and LASL/TD multigroup structures. Neutron interaction cross sections were obtained by collapsing data from the 14-element, 100-group LASL/CTR library and the 40-element, 30-group LASL/TD library into the 25-group structure. The resulting data set is being used in the design of fusion-fission reactors based on the ^{238}U - ^{239}Pu cycle, which might be called "fast hybrids."

A second group-collapsed data set was produced for the analysis of fusion-fission hybrid reactors based on the ^{232}Th - ^{233}U cycle in a graphite lattice (thermal hybrids). This library consists of data for all of the elements contained in the 25-group fast library, collapsed to a new 19-group format, including 3 upscatter groups. In addition, cross-section sets were prepared for ^{232}Th, ^{233}Pa, and ^{233}U by processing ENDF/B data with MC^2 (Ref. 7). Also,

9

a special set for ^{12}C was prepared by combining data from MC^2 and the thermal upscatter code, FLANGE.[14]

In the area of nuclear data uncertainty analysis, the available data for the ^{94}Nb(n,γ) have been reviewed. Alternative cross-section sets have been prepared for this reaction which, while consistent with the available data, are significantly different at neutron energies above 50 eV. This effect produces 10-20% uncertainties in afterheat and activation calculations[20] for the Reference Theta Pinch Reactor.

The United States Nuclear Data Committee CTR Subcommittee met in San Diego on April 15, immediately preceding the First Topical Meeting on the Technology of Controlled Nuclear Fusion. Of the actions placed on LASL during this meeting, the CTR reviews of the ENDF/B-IV evaluated data files for H, ^{6}Li, ^{7}Li, N, O, and Al were completely rewritten and forwarded to the Subcommittee Chairman. Tables of "estimated" but uncorrelated errors were attached to each review. These CTR reviews from all the laboratories already have been assembled and will soon be distributed by ORNL.

In anticipation of the need for more radioactive decay data, users in the fusion, fission, and weapons areas are currently being polled to determine whether an ENDF/B type format could be developed which would contain the information needed for the majority of radioactivity and heating calculations. At the suggestion of DCTR, the USNDC list of measurement requests (USNDC-6) was reviewed and three new requests suggested. USNDC-6 is now scheduled for review and updating this fall by the CTR Subcommittee.

VI. R-MATRIX ANALYSIS OF REACTIONS IN THE ^{17}O SYSTEM (G. M. Hale, P. G. Young, and D. G. Foster, Jr.)

Cross sections for the scattering of neutrons from ^{16}O are important for calculating neutron transport in air and other materials of interest in shielding designs and weapons effects studies. We have carried out a comprehensive R-Matrix analysis of reactions in the ^{17}O system which includes the neutron cross sections of interest in addtion to data from the ^{16}O(n,α)^{13}C and ^{13}C(α,α)^{13}C reactions. The analysis confirmed that most of the data analyzed were consistent with the currently accepted level scheme for ^{17}O, and the results were incorporated in the oxygen evaluation contained in the Military Applica-

tions Nuclear Data Library (MANDL) and in Version IV of the Evaluated Nuclear Data File (ENDF/B).

As part of our continuing responsibility to upgrade evaluations for the Defense Nuclear Agency, we are currently investigating the few isolated regions in which agreement between the analysis described above and experiment was not completely satisfactory. The disagreement was evident mainly in the differential cross sections, indicating possibly incorrect level assignments in these regions. Alternative assignments are being explored in regions around 3.8, 4.3, and 4.5 MeV neutron energy. In the vicinity of 3.8 MeV, we are aided by the existence of new polarization measurements from Yale.[21] Although the changes in the neutron cross sections resulting from this investigation are not expected to be extensive, they will be incorporated in an update of the current MANDL evaluation.

VII. R-MATRIX ANALYSIS OF REACTIONS IN THE ^{11}B SYSTEM (G. M. Hale and P. G. Young).

Neutron cross sections for the ^{10}B are important in the design of reactors and thermonuclear devices, as well as in the area of neutron cross-section measurement. Even at relatively low energies, the large spin of ^{10}B introduces many scattering amplitudes that must be determined in analyzing n-^{10}B data. For this reason, the R-matrix analysis that was used to provide n-^{10}B cross sections at low energies in the ENDF/B-IV evaluation included a variety of data for a number of reactions in the ^{11}B system. Indications were that unidentified levels in ^{11}B, which are evident mainly in the α-^{7}Li cross sections, do affect the neutron cross sections to some extent. Since these effects could be significant for cross sections used as neutron standards, we are attempting to complete the knowledge about the level structure of ^{11}B in the region of interest, and determine the effect of these levels on the neutron cross sections.

Since most of the width in these levels appears to occur in the α-channels, we have performed a separate analysis of data measured for the ^{7}Li(α,α)^{7}Li and ^{7}Li(α,α')^{7}Li* reactions by Cusson.[22] The fit resulting from preliminary level assignments to the ^{7}Li(α,α')^{7}Li* integrated cross section between E_α = 2.8 and 6.3 MeV is shown in Fig. 13. Of these resonances, only the 5/2- at E_α ~ 5 MeV has been identified in the neutron data.[23] Cusson attempted assign-
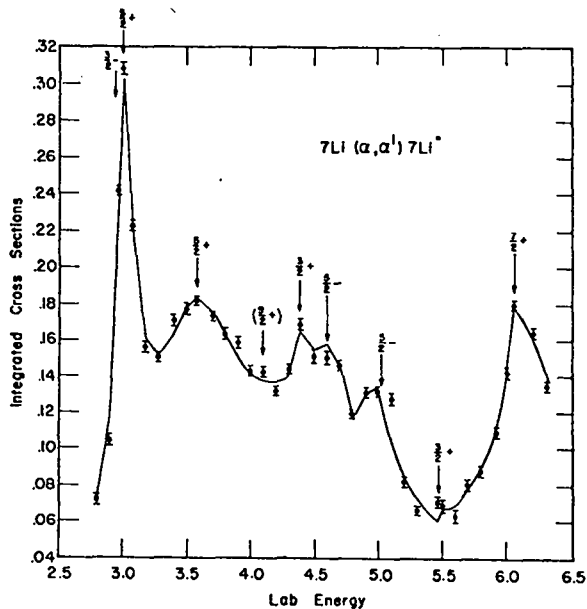
Fig. 13. Fit (solid line) to the integrated
$^7\text{Li}(\alpha,\alpha')^7\text{Li*}$ cross section measured
by Cusson between $E\alpha = 2.8$ and 6.3 MeV.
The arrows mark tentative assignments
made for the resonances.

ments for a few of the levels below the neutron
threshold ($E_\alpha = 4.4$ MeV). The present analysis ap-
pears to disagree even with his most definite as-
signment, a 7/2+ for the level at 3.03 MeV. Figures
14-15 show the fit to selections of the $^7\text{Li}(\alpha,\alpha)^7\text{Li}$
and $^7\text{Li}(\alpha,\alpha')^7\text{Li}^*$ differential cross sections, re-
spectively, for the level scheme shown in Fig. 13.

Although these results are preliminary, the
7/2+ resonance at 6.06 MeV and the interfering 5/2-
resonances at 4.6 and 5.0 MeV appear to be well es-
tablished by the data. It remains to examine the
effect of these resonances and the others upon the
cross sections for neutron induced reactions on ^{10}B.

VIII. MISCELLANEOUS EVALUATION AND REVIEW ACTIVITIES
(L. Stewart, P. G. Young, D. G. Foster, Jr.
and G. F. Auchampaugh [P-3])

In addition to making miscellaneous checks,
corrections, and additions in evaluations of some of
the fissile and fertile materials, we have during
this quarter edited and reviewed ENDF/B-IV evalua-
tions for Fe and for the ^{238}U γ-production (prompt
gammas only) cross sections. A significant amount
of effort was also invested in helping update and
correct the ENDF/B Procedures Manual, since Brook-
haven National Laboratory specifically requested com-
ments from each laboratory in preparation for issuing

a new users' guide. At the request of DRRD and DNA,
some of the requests for measurements in USNDC-6 were
reviewed and forwarded, with comments and new requests,
to the appropriate agencies.

IX. NASA EXTENSION OF MEDIUM-ENERGY NUCLEAR-DATA
LIBRARY (D. G. Foster, Jr. and D. R. Harris)

The problems in the EVAP module of CROIX which
were discussed last quarter have been resolved and
solutions have been flow-charted. Energy-imbalance
problems that occur in EVAP are a by-product of a
rather haphazard treatment of the reaction kinemat-
ics. An analytically correct method of forcing emis-
sion near threshold is also being incorporated.

A proper solution to the "energy-overshoot"
problem in the intranuclear-cascade module appears
infeasible in the time available. Accordingly, a
simple energy-scaling correction will be applied and
the evaporation aborted when this pathology develops.
If time permits, we hope to explore the running-time
penalty involved in using the Tausworthe algorithm
instead of our present random-number generator. The
present generator (which is short enough to be coded
in-line) has been shown to have marked short-range
correlation, which may account for some of the start-
ling bunching of transparencies in the intranuclear-
cascade histories.

X. TESTING OF NUCLEAR DATA OF IMPORTANCE IN SHIELD-
ING APPLICATIONS AGAINST INTEGRAL EXPERIMENT
(D. W. Muir and R. J. LaBauve)

Work continues on the development of benchmark
specifications for the ZPPR/FTR-2 shield experiment.[24]
In a paper[25] describing our calculation of the gamma-
ray dose distribution, it was noted that resonance
self-shielding effects are quite important in the
ZPPR/FTR-2, especially in the "depleted zone," where
most of the gamma-ray production proceeds via the
$^{238}\text{U}(n,\gamma)$ reaction. For this reason we have repeated
the gamma-ray calculation using self-shielded gamma-
ray production cross sections in all regions. Zone-
dependent, self-shielded, multigroup neutron cross
sections were generated for all gamma-producing re-
actions using MC^2 (Ref. 7). These multigroup cross
sections were then input to LAPHANO[26] to produce the
self-shielded gamma-ray production matrices. The
resulting gamma-ray flux distribution was calculated
with TWOTRAN.[27] This flux was converted to thermo-
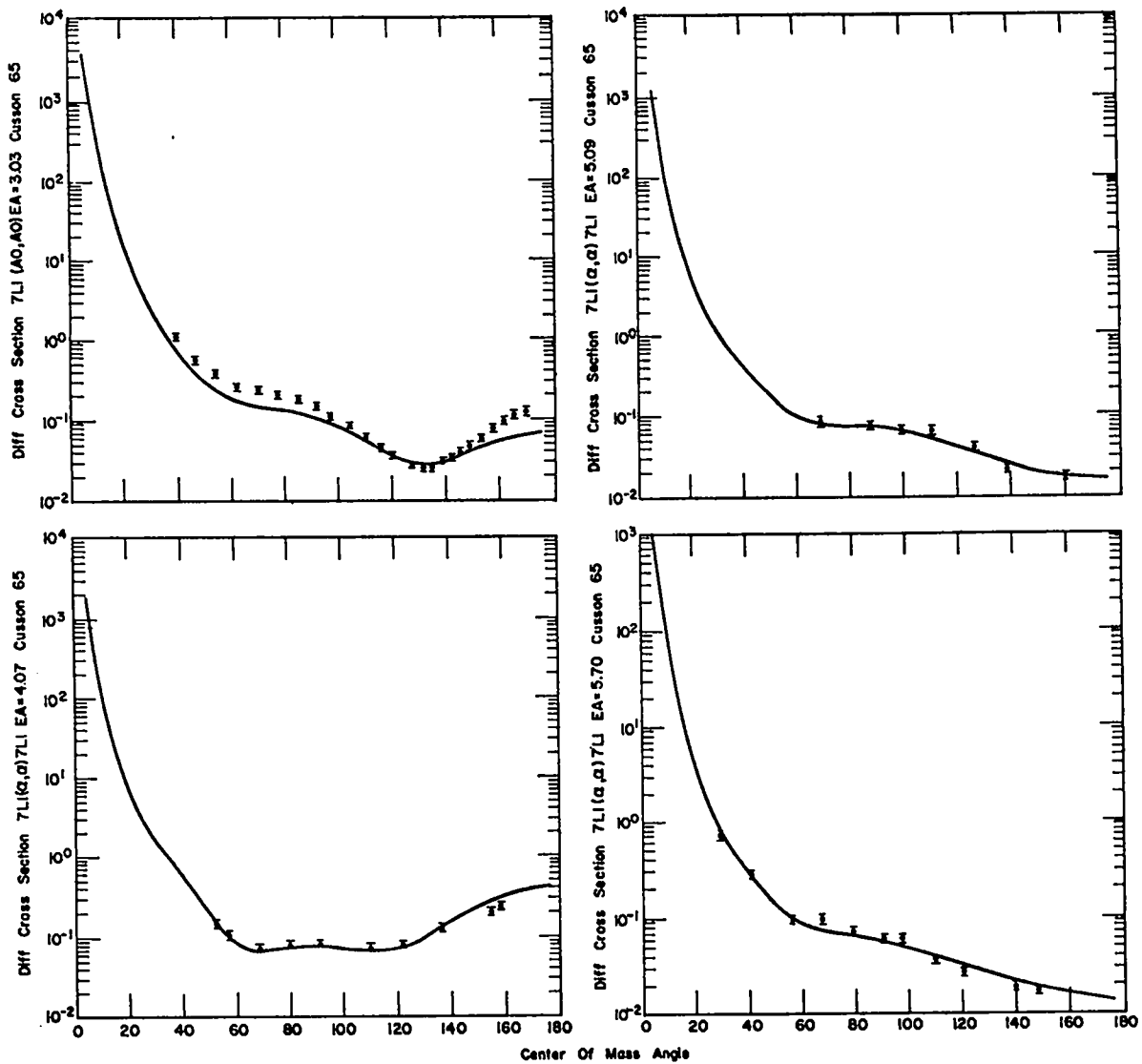luminescent dosimeter (TLD) absorbed dose, and the

11

Fig. 14. Fit (solid line) to selected ^{7}Li$(\alpha,\alpha)^7$Li angular distributions measured by
Cusson, using the level scheme of Fig. 13.

results are compared with experiment in Fig. 16.
The upper two calculated curves include corrections
for the cavity-ionization effect[28] and TLD neutron
sensitivity,[29] respectively.

Inclusion of the self-shielding effect lowers
the previous results[25] by about a factor of two in
the depleted zone and by about 20% in the sodium-
steel shield. The agreement between calculation and

experiment is now quite good, except at large radii.
The discrepancy there is due to undercalculation of
the neutron flux, as shown by the results for the
^{238}U and ^{239}Pu fission traverses discussed in Ref.
25. We conclude that the gamma-ray production data
in ENDF/B are adequate for survey calculations (with
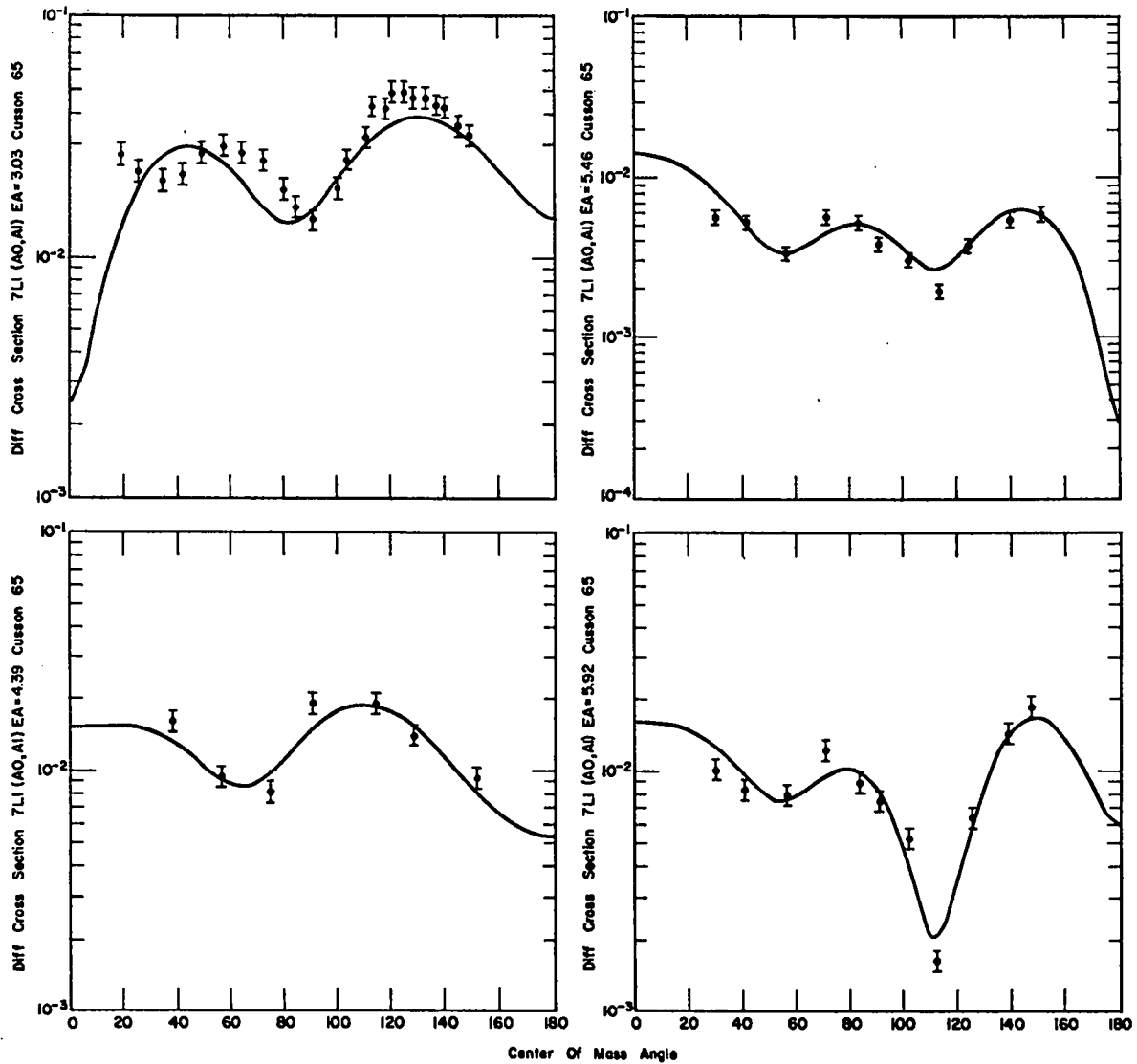an accuracy of about 20%) in this type of assembly.

Fig. 15. Fit (solid line) to selected ^{7}Li(α,α') ^{7}Li* angular distributions measured by Cusson, using the level scheme of Fig. 13.

XI. CINDER-7 AND RELATED CODING (T. R. England and N Whittemore)

The major options of CINDER-7 have been debugged. The γ-spectrum routine is working successuully as are the data management routines. Work on further program changes continues. The 34 subroutines require 18630_{10} memory locations. Data storage is variably dimensioned and depends on the type of calculation.

A program to read data decks in the older versions of CINDER and repunch cards in the free form input for CINDER-7 is operational. This will be further modified to process ENDF/B-IV data.
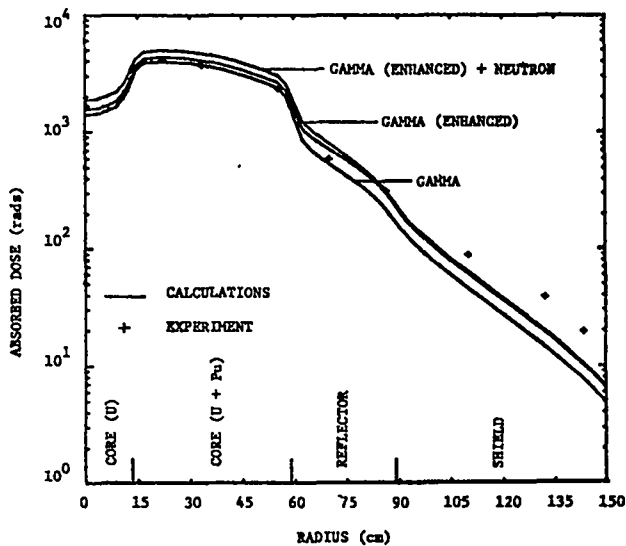
Fig. 16. Measured and calculated TLD response in ZPPR/FTR-2 for a central traverse.

REFERENCES

1. G. M. Hale, D. R. Harris, and R. E. MacFarlane, "Applied Nuclear Data Research and Development Quarterly Progress Report for the period January 1 through March 31, 1974," Los Alamos Scientific Laboratory LA-5655-PR (1974).

2. C. R. Weisbin and R. J. LaBauve, "Specifications of a Generally Useful Multigroup Structure for Neutron Transport," Los Alamos Scientific Laboratroy report LA-5277-MS (1973).

3. J. C. Vigil, "Service Modules for Version II Standard Interface Data Files," Los Alamos Scientific Laboratory report LA-5367-MS (1973).

4. M. Raymund, "TEDIUM: Idealized Neutron Data for Testing Library Processing Codes," ANS Reactor Physics Division Topical Meeting on New Methods in Reactor Physics, CONF-720901, p. 1048 (1972)

5. M. K. Drake, "Data Formats and Procedures for the ENDF/B Neutron Cross Section Library," Brookhaven National Laboratory report BNL-50274 (T-601)(TID-4500) ENDF-102, Vol. I (1970).

6. D. E. Cullen, "Program SIGMA1," (Version 74-1) Lawrence Livermore Laboratory report UCID-16426 (1974).

7. B. J. Toppel, A. L. Rago, and D. M. O'Shea, "MC^2, A Code to Calculate Multigroup Cross Sections," Argonne National Laboratory report ANL-7318 (1967).

8. G. N. Paik, Westinghouse Advanced Reactor Division, private communication.

9. C. R. Weisbin, P. D. Soran, D. R. Harris, R. J. LaBauve, and H. S. Hendricks, "MINX – A Multigroup Interpretation of Nuclear X-Sections," Trans. Am. Nucl. Soc. 16, 127 (June 1973).

10. O. Ozer, Ed., "Description of the ENDF/B Processing Codes and Retrieval Subroutines," Brookhaven National Laboratory report BNL-50300 (ENDF 11) (June 1971).

11. D. M. Green and T. A. Pitterle, "ETOE, A Program for ENDF/B to MC^2 Data Conversion," Atomic Power Development Associates, Inc. report APDA-219 (ENDF-120) (1968).

12. W. W. Clendenin, "Calculation of Thermal Neutron Scattering Cross Sections for Crystalline Materials: The TOR Program," Los Alamos Scientific Laboratory report LA-3823 (1967).

13. W. W. Clendenin, "Calculation of Thermal Neutron Diffusion Length and Group Cross Sections: The GLEN Program," Los Alamos Scientific Laboratory report LA-3893 (1968).

14. H. C. Honeck and D. R. Finch, "FLANGEII (Version 71-1) A Code to Process Thermal Neutron Data from an ENDF/B Tape," E. I. DuPont De Nemours and Co. Savannah River Laboratory report DP-1278 (1971).

15. J. U. Koppel, J. R. Triplett, and Y. D. Naliboff, "GASKET, A Unified Code for Thermal Neutron Scattering," General Atomic report GA-7417 (1966).

16. Preliminary Safety Analysis Report, Fulton Generating Station Units 1 and 2, Philadelphia Electric Company (1973).

17. T. R. England, G. L. Hartfield, and R. K. Deremer, "Xenon Spatial Stability in Large Seed-Blanket Reactors," Bettis Atomic Power Laboratory report WAPD-T-M-606 (1967).

18. D. R. Harris and P. S. Lacey, "A Simple Approximate Test for Spatial Xenon Instability," Trans. Am. Nucl. Soc. 3, 437 (1960).

19. R. Sund et al., "Afterheat Calculations for the HTGR," General Atomic report GA-A-12499 (GA-LTR-4) (Nov. 1973).

20. Donald J. Dudziak, private communication

21. G. T. Hickey et al., "Polarization of Neutrons Elastically Scattered from ^{16}O," Phys. Lett. 47B, 348 (1973).

22. R. Y. Cusson, "A Study of the Elastic and Inelastic Scattering of Alpha Particles by Lithium-7," Thesis, California Institute of Technology (1965).

23. R. O. Lane et al., "^{11}B States Observed in the Scattering of Neutrons from ^{10}B and in the $^{10}B(n,\alpha)^7Li$ Reaction," Phys. Rec. C4, 380 (1971).

24. A. Travelli, "FFTF Critical Assembly Experiments—Planning and Evaluation," Argonne National Laboratory report ABL-7669, p 17 (1970).

25. D. W. Muir and R. J. LaBauve, "Analysis of ZPPR/FTR-2 TLD Measurements Using ENDF/B-III Data," Am. Nucl. Soc. 18, 395 (1974).

26. D. J. Dudziak, R. E. Seamon, and D. V. Susco, "LAPHANO: A P_0 Multigroup Photon-Production Matrix and Source Code for ENDF," Los Alamos Scientific Laboratory report LA-4750-MS (ENDF-156) (1967).

27. K. D. Lathrop and F. W. Brinkley, "Theory and Use of the General Geometry TWOTRAN Program," Los Alamos Scientific Laboratory report LA-4432 (1970).

28. G. G. Simons and T. J. Yule, "Gamma-Ray Heating Measurements in Zero-Power Fast Reactors with Thermoluminescent Dosimeters," Nucl Sci. and Eng. 53, 162 (1974).

29. C. L. Wingate, E. Tochilin, and C. Goldstein, "Response of Lithium Fluoride to Neutrons and Charged Particles," Proc. Con. Luminescence Dosimetry (Stanford) (June 21-23, 1965).

PUBLICATIONS

1. G. M. Hale et al, "An R-Matrix Analysis of p-^{3}He Elastic Scattering Below E_p = 19.5 MeV," Bull. Am. Phys. Soc. 19, 506 (1974).

2. G. M. Hale, P. G. Young, and R. A. Nisley, "R-Matrix Analysis of the n + ^{10}B System at Low Energies," Trans. Am. Nucl. Soc. 18, 327 (1974).

3. G. M. Hale, P. G. Young, and D. G. Foster, Jr., "R-Matrix Analysis of the ^{17}O System, ENDF/B-IV," Trans. Am. Nucl. Soc. 18, 366 (1974).

4. G. M. Hale, "R-Matrix Analysis of Reactions in Light Nuclei," Seminar presented at Ohio State University, Columbus, Ohio, April 1974.

5. D. W. Muir, "Nuclear Data for Fusion Reactor Blanket Neutronics," Seminar at University of Florida, Gainesville, Feb. 1974; North Carolina State University, Raleigh, Feb. 1974; and Georgia Insititue of Technology, Atlanta, Feb. 1974.

6. D. W. Muir, "Sensitivity of Neutron Multigroup Cross Sections to Thermal Broadening of the Fusion Peak," to be published in the Proceedings of the First Topical Conference on the Technology of Controlled Nuclear Fusion, San Diego, April 1974.

7. P. D. Soran, D. J. Dudziak, and D. W. Muir, "Effects of Be(n,2n) Multigroup Treatment on Theta-Pinch Blanket Nucleonics," to be published in the Proceedings of the First Topical Conference on the Technology of Controlled Nuclear Fusion, San Diego, April 1974.

8. D. W. Muir and R. J. LaBauve, "Analysis of ZPPR/FTR-2 TLD Measurements Using ENDF/B-III Data," Trans. Am. Nucl. Soc. 18, 395 (1974).

9. D. R. Harris, Ed., "Applied Nuclear Data Research and Development Quarterly Progress Report for the period July 1 through September 30, 1973," Los Alamos Scientific Laboratory report LA-5546-PR (April 1974).

10. G. M. Hale, D. R. Harris, and R. E. MacFarlane, Eds., "Applied Nuclear Data Research and Development October 1 through December 31, 1973," Los Alamos Scientific Laboratory report LA-5570-PR (April 1974).

11. G. M. Hale, D. R. Harris, and R. E. MacFarlane, Eds., "Applied Nuclear Data Research and Development Quarterly Progress Report for the Period January 1 through March 31, 1974," Los Alamos Scientific Laboratory report LA-5655-PR (July 1974).

12. D. R. Harris, "Consistency Among Differential Nuclear Data and Integral Observations," Trans. Am. Nucl. Soc. 18, 340 (1974).

13. T. R. England and D. R. Harris, "Integral Tests of Fission Product Data Files," Trans. Am. Nucl. Soc. 18, 331 (1974).

ALT:160(130)